Kalman Filter Based Estimation of Ionic Concentrations and Gating Variables in a Cardiac Myocyte Model

Laura M Muñoz, Niels F Otani

School of Mathematical Sciences, Rochester Institute of Technology, Rochester, USA

Abstract

The purpose of this study is to give researchers improved access to important electrophysiological quantities, such as ion-channel gating variables, that are difficult or impossible to measure during in vitro experiments, yet are thought to be critical to the formation of dangerous arrhythmias. To help fulfill this goal, we examined the feasibility of inferring these types of quantities from more readily available data, such as measurements of cellular membrane potential. First, we performed an observability analysis on a linearized Luo-Rudy dynamic (LRd) myocyte model, which showed that concentration and gating variables in the LRd model can be reconstructed from membrane potential data. Next, we designed a Kalman filter for the model and tested its performance under simulated conditions. The tests demonstrated the ability of the filter to produce more accurate estimates of the system state compared to the case without measurement feedback. This research is relevant to human health, since state estimation methods such as Kalman filtering could be used to obtain more information about the response of a single cell to the influence of pharmacological agents or other anti-arrhythmic therapies, over a larger range of cellular variables than are typically monitored during an in vitro study.

1.   Introduction

To gain a better understanding of the causes of abnormal cardiac rhythms, researchers have relied on a variety of measurement methods, including electrocardiography, optical mapping, electrode recordings, and patch clamping. While these approaches can provide valuable information, it is generally difficult or impossible to obtain direct, concurrent observations of all processes, such as ion-channel gating behavior and intracellular Ca^{2+} dynamics, that are thought to be important to arrhythmogenesis.

To allow for a more complete view of electrophysiological variables and their interactions during arrhythmia formation, we have investigated state estimation algorithms as a means of using available data to reconstruct quanti-ties that are difficult or impossible to observe in an *in vitro* setting. Previously, we demonstrated that microelectrode-based membrane potential data can be used to estimate a refractory variable, in addition to membrane potentials at unmonitored locations within a cardiac fiber [1]. In this study, we applied observability analysis and Kalman filtering methods [2] to a more physiologically realistic cell model, the Luo-Rudy dynamic (LRd) model [3, 4]. The feasibility of estimating gating and other variables from membrane potential measurements has been corroborated by other studies where Kalman filters, nonlinear filters, or closed-loop observers were applied to lower-order models of cardiac fibers and neurons [5–7]. However, to our knowledge, these methods have not been tested on cardiac ion-channel models, such as the LRd model, which include direct representations of intracellular ionic concentrations and Ca^{2+} dynamics. These models offer a wider range of variables that can be compared directly with measurements, and may serve as a basis for estimation methods that improve our understanding of the mechanisms of arrhythmias.

2.   Methods

The Luo-Rudy dynamic (LRd) myocyte model [3, 4] was selected for this study since it represents ionic behavior, including intracellular Ca^{2+} dynamics, in a physiologically realistic manner while still having a relatively small number of state variables. The $N = 17$ state variables include the membrane potential V (mV) and gating variables h, m, j, d, f, x_r, x_{s1}, x_{s2}, b, g. Additional variables are the following ionic concentrations (mmol/L): the intracellular Na^+ concentration, $[Na^+]_i$, the intracellular K^+ concentration, $[K^+]_i$, the total concentration of free and buffered intracellular Ca^{2+}, $[Ca^{2+}]_{i,t}$, the total Ca^{2+} concentration in the junctional sarcoplasmic reticulum (SR) $[Ca^{2+}]_{j,t}$, and the Ca^{2+} concentration in the network SR, $[Ca^{2+}]_n$. Another state variable, I_{rel} (mmol/L per ms), represents the Ca^{2+} release from the junctional SR to the myoplasm. Defining the state vector as $X(t) = [V\ h\ m\ j\ d\ f\ x_r\ [Ca^{2+}]_{i,t}\ [Na^+]_i\ [K^+]_i\ [Ca^{2+}]_{j,t}\ ... [Ca^{2+}]_n\ x_{s1}\ b\ g\ x_{s2}\ I_{rel}]^T(t)$, the cell dynamical equa-

tion has the form $\dot{X}(t) = f(X(t), i_{\text{stim}}(t))$, where i_{stim} is the stimulus current. A more complete description of the model is available in [4].

Simulation codes for the LRd model were downloaded from the Rudy Lab website [4, 8]. A conservative biphasic stimulus current was applied periodically to the cell model, and the inter-stimulus interval, called the basic cycle length (BCL), was set to 1000ms. We assumed that certain state variables were measured periodically at times $t_m + jBCL$, and that stimuli were applied at times $t_s + jBCL$, $j \in \{0, 1, \ldots\}$. The LRd model was integrated using a forward-Euler method with a time step of Δt = 0.005ms. Matlab was used to perform all computations.

For an integration interval of one BCL, fixed points X_o of the time-integrated LRd model were estimated with a Newton-Krylov solver [9]. Corresponding Jacobians were computed with finite difference methods [9], with the added step of taking a central difference to reduce the effect of fixed-point estimation errors on the Jacobian [10]. Eigenvalues were determined with the `eig` function in Matlab.

The resulting linearized model had the form

$$x(j + 1) = A(t_m - t_s)x(j)$$
$$y(j) = Cx(j)$$

where $x(j) = x(t_m + jBCL) = X(j) - X_o(t_m - t_s)$ is the state vector for the linearized system. $A(t_m - t_s)$ and $X_o(t_m - t_s)$ are the Jacobian matrix and fixed point obtained for a particular choice of offset between the stimulus and measurement times. The output y is the source of measurements $y(0)$, $y(1)$, …, which are related to the state vector through the output matrix C. For simplicity we assumed that no perturbations were applied to the stimulus current.

To determine whether measurements of any individual variable were sufficient to estimate the remaining variables, we analyzed a model property called observability. Each of the state variables was considered in turn as a possible source of data, leading to a collection of N output matrices of size $1 \times N$ of the form $C_i = [0 \ldots 0 \, 1 \, 0 \ldots 0]$, where i^{th} element is 1, indicating that the ith variable was the measured variable. For each output matrix, the observable and unobservable subspaces were computed using the `obsvf` function in Matlab. Our analysis made use of a well-known result in linear systems theory, that if a system is observable from a particular output, then that output is sufficiently informative to allow finite-time reconstruction of a previous state of the system, provided that the history of inputs to the system is also known.

To set up a standard Kalman filter design problem, we assumed that the system was affected by two noise signals,

the process noise $w(j)$ and measurement noise $v(j)$:

$$x(j + 1) = A(t_m - t_s)x(j) + B_w w(j)$$
$$y(j) = Cx(j) + v(j)$$

where $w(j)$, $v(j)$, and the initial state $x(0)$ are independent and Gaussian-distributed, and $w(j)$ and $v(j)$ are zero-mean scalar white noise signals with variances Q and R. We assumed that the process noise affected the membrane potential dynamics through $B_w = [1 \ 0 \ \ldots \ 0]^T$. Since the system is time-invariant for fixed $t_m - t_s$, if it is also observable (or at least detectable, meaning that all of the unobservable eigenvalues are stable) for some choice of C and satisfies certain restrictions involving the noise terms, a steady-state Kalman filter exists and is well-defined.

Using the `kalman` function in Matlab, we designed a Kalman filter of the form

$$\hat{x}(j + 1|j) = A(t_m - t_s)\hat{x}(j|j - 1)$$
$$+ L(y(j) - C\hat{x}(j|j - 1)),$$

where $\hat{x}(j|j - 1)$ is the state estimate at cycle j, based on all past measurements up to $y(j - 1)$, and L is the Kalman filter gain matrix. The estimation error was defined as $e(j|j - 1) = x(j) - \hat{x}(j|j - 1)$. To verify the basic functionality of the filter, we simulated the open-loop ($L = 0$) and closed-loop estimation errors with a random initial condition, with w and v chosen as sequences of zero-mean Gaussian-distributed pseudorandom numbers, and checked the behavior of the filter using different settings for the process and measurement noise variances.

3.   Results

The eigenvalues of the linearized LRd model were computed and are displayed in Fig. 1. To three decimal places, the leading eigenvalues are $\lambda_1 = 1.000$, $\lambda_2 = 0.990$, and $\lambda_3 = 0.717$. The eigenvector of λ_1 is primarily in the direction of $[K^+]_i$, the second eigenvalue is mainly associated with and $[K^+]_i$ and $[Na^+]_i$, and the third mode has its largest component along $[Ca^{2+}]_{j,t}$. The remaining eigenvalues are relatively close to the origin.
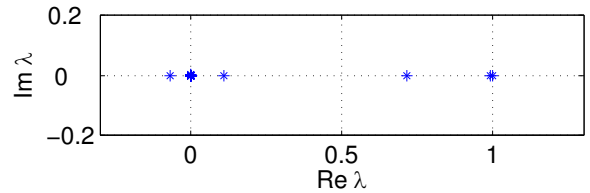

Figure 1.   Eigenvalues of the linearized LRd model, for BCL = 1000ms.

An example of the results of the observability analysis is shown in Fig. 2 for $t_m - t_s = 1000 - \Delta t$ ms. The eigenvalue magnitudes are plotted against the measured variable index derived from the ordering of variables in the state vector $X(t)$, e.g. $i = 1$ ($C = C_1$) corresponds to measuring $V(j)$, $i = 2$ corresponds to measuring $h(j)$, etc.
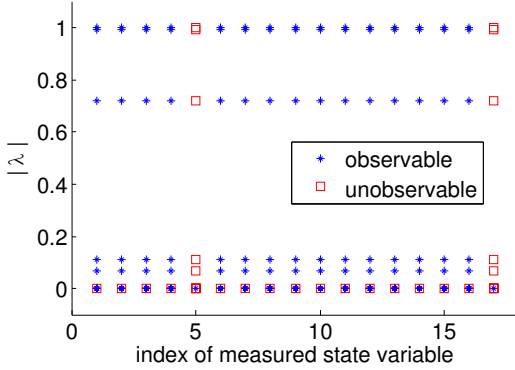

Figure 2. Eigenvalue magnitudes vs. index of measured state variable, showing observable and unobservable modes, for $t_m - t_s = 1000 - \Delta t$ ms.

As seen in Fig. 2, for a measurement taken $1000 - \Delta t$ ms after the application of the stimulus, the larger eigenvalues are observable from measurements of each of the state variables except for $i = 5$ (d, the activation gate of $I_{Ca(L)}$), and $i = 17$ (I_{rel}). For each choice of output, one or more of the eigenvalues near the origin is unobservable, as indicated by the row of squares near $|\lambda| = 0$. Since these eigenvalues are highly stable, this loss of observability will not pose a problem in our estimator design; we are mainly concerned with the eigenvalues near the stability boundary, which only become unobservable when the output is d or I_{rel}. Observability properties for additional $t_m - t_s$ values are summarized in Table 1.

Table 1. Observability of larger LRd eigenvalues ($|\lambda > 0.06|$) for different values of $t_m - t_s$. The second column lists any outputs from which the larger eigenvalues were unobservable.

$t_m - t_s + \Delta t$ (ms)	Not observable from
200	d
400	d, I_{rel}
600	d, I_{rel}
800	d, I_{rel}
1000	d, I_{rel}

For the timings shown in Table 1, the larger eigenvalues were found to be observable from measurements of the majority of the state variables, including V. Only d,

and for the last four intervals tested, I_{rel}, were found to be insufficient for observability of the larger modes.

To further investigate the proposed estimation method, a Kalman filter was designed for $t_m - t_s = 1000 - \Delta t$ ms, assuming that only noise-contaminated measurements of V were available. We selected $Q = 0.01$ and tested two settings for the measurement noise, $R = 0.001$ and $R = 0.1$. Simulation results for the open-loop ($L = 0$) estimation errors are shown in Fig. 3, and the Kalman filter estimation errors are shown in Fig. 4, for the case $Q = 0.01$, $R = 0.001$. For clarity, errors are only displayed for a few variables in each figure; the remaining errors have similar magnitudes.
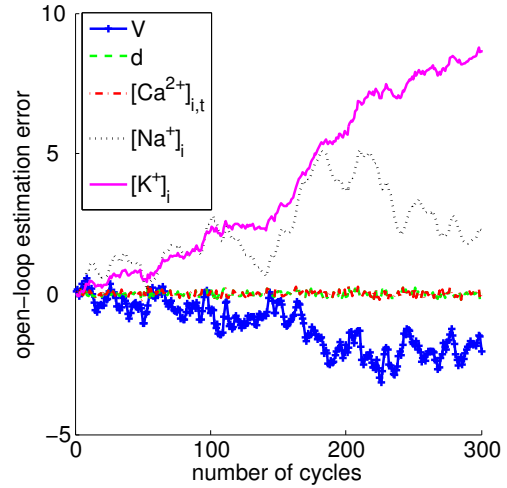

Figure 3. Open-loop estimation errors vs. cycle number for selected state variables.

For the random noise settings used in Figs. 3 and 4, the estimation error covariance norm over 300 cycles was 9.88 for the open-loop case, 6.46 (34.6% smaller than the open-loop norm) for the Kalman filter with $Q/R = 10$, and 7.18 (27.3% smaller than the open-loop norm) for the Kalman filter with $Q/R = 0.1$.

4. Discussion and conclusions

The results of the observability analysis and Kalman filter design demonstrated the overall feasibility of reconstructing cellular dynamical variables, such as ionic concentrations and gating states, from measurements of the membrane potential. The loss of observability when d or I_{rel} was chosen as the output presumably reflects a weak influence of the other variables on the dynamics of d and I_{rel}, and further investigation of these results may produce more detailed physiological interpretations. Expanding
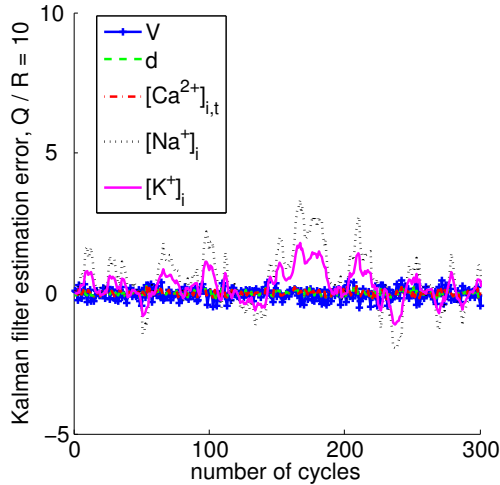
Figure 4. Kalman filter estimation errors vs. cycle number for selected state variables.

upon our study, by including a finer-grained exploration of $t_m - t_s$ values, a wider range of BCLs, different observability measures, and variations on variable scalings and rank tolerances may reveal additional insights into which choices of output variables are best suited for state estimation.

The large drift in the open-loop estimation errors in Fig. 3 was caused by the $[K^+]_i$ memory mode at the stability boundary. The Kalman filter reduced the largest eigenvalue to approximately $\lambda = 0.992$ for both of the tested Q/R ratios, and produced smaller estimation errors as shown in Fig. 4. It was determined (results not shown due to space constraints) that the leading Kalman filter eigenvalue-eigenvector pair is similar in size and direction as the second open-loop mode (associated with $[K^+]_i$ and $[Na^+]_i$) for both Q/R ratios, which implies relatively weak observability of this mode as compared with $\lambda_1 = 1.000$. As expected, the improvement in the estimation error covariance was larger for $Q/R = 10$, which corresponds to having data that is of higher quality than the model predictions. Topics of ongoing work include modeling the noise terms in a more realistic manner, developing reduced-order and predictor-corrector variants of the filter, and testing the estimator with data from real cells.

In summary, our analysis of the LRd model has shown that membrane potential data can be used to estimate other quantities, such as gating and ionic variables, which may be difficult to measure but are thought to play an important role the development of arrhythmias. Closed-loop estimation methods such as the Kalman filter constitute a promising approach for allowing researchers to use limited data to gain a more complete understanding of the dynamical behavior of cardiac ion-channel quantities.

Acknowledgements

References

[1] Muñoz LM, Otani NF. Enhanced computer modeling of cardiac action potential dynamics using experimental data-based feedback. Computing in Cardiology 2010;37:837–840.

[2] Kalman RE. A new approach to linear filtering and prediction problems. Transactions of the ASME Journal of Basic Engineering 1960;82(Series D):35–45.

[3] Luo CH, Rudy Y. A dynamic model of the cardiac ventricular action potential. I. Simulations of ionic currents and concentration changes. Circ Res 1994;74:1071–1096.

[4] Livshitz L, Rudy Y. Uniqueness and stability of action potential models during rest, pacing, and conduction using problem-solving environment. Biophys J 2009;97:1265–1276.

[5] Garzón A, Grigoriev RO, Fenton FH. Model-based control of cardiac alternans in Purkinje fibers. Phys Rev E 2011;84:041927–1–12.

[6] Ullah G, Schiff S. Tracking and control of neuronal Hodgkin-Huxley dynamics. Phys Rev E 2009;79:040901–1–4.

[7] Kobayashi R, Tsubo Y, Lansky P, Shinomoto S. Estimating time-varying input signals and ion channel states from a single voltage trace of a neuron. Advances in Neural Information Processing Systems 2011;24.

[8] Rudy Y. Rudy laboratory website. http://rudylab.wustl.edu/research/cell/code/Livshitz_LRd_Strand_2009.zi%p. Accessed: 2011-05-20.

[9] Kelley CT. Solving Nonlinear Equations with Newton's Method. Number 1 in Fundamentals of Algorithms. Philadelphia: SIAM, 2003.

[10] Li M, Otani NF. Ion channel basis for alternans and memory in cardiac myocytes. Ann Biomed Eng 2003;31:1213–1230.

Address for correspondence:

Laura Muñoz
Rochester Institute of Technology
85 Lomb Memorial Drive
Rochester, NY, 14623
laura.m.munoz@gmail.com